Evaluating Storage and Effective Moduli of In Situ Polymerised and Melt Extruded PA6 Graphite (G) Composites

Muneer Umar[1], Michael Ikpi Ofem[2*], Auwal Sani Anwar[1], Muhammad Murtala Usman[3]

[1]Chemical Engineering Department, Kaduna Polytechnic, Nigeria
[2]Mechanical Engineering Department, Cross River University of Technology Calabar, Nigeria
[3]Chemical Engineering Department, Federal Polytechnic, Nasarawa, Nigeria
**Corresponding author: michaeliofem@crutech.edu.ng*

ABSTRACT

Four PA6/graphite (G) composites systems were made. Two using in situ polymerisation equivalent in mixing strain and two systems melt extrusion of equivalent processing strain. The effective modulus of the carbons, room temperature storage modulus and storage modulus at 80 ºC were evaluated. The composite/unfilled PA6 ratios at E25 and that at E80 for the in situ polymerised system IG 40/10 are 1.37 and 1.63, respectively. For the in situ polymerised system IG 20/20, the same were 1.96 and 2.28, respectively. For the melt-extruded systems, G 100/6 had the best E25 ratio of 1.67 and E80 of 2.03, whereas the same for G 200/3 system were respectively 1.87 and 2.64. While the better storage modulus properties exhibited by IG 20/20 in the in situ polymerised system is associated with a better filler connectivity network that enhanced heat dissipation. The better values shown in the G 200/3 melt-extruded system is associated with the lesser extrusion, which significantly reduced the tendency to thermal decay. Effective modulus for the in situ polymerised systems IG 40/10 and IG 20/20 were 7.5GPa and 8.9GPa while that of melt-extruded systems G200/3 and G100/6 tallied at 8.2 GPa.

Keywords: *Effective-modulus, in situ-polymerisation, melt-extrusion, storage-modulus*

I. Introduction

Research on polymer nano-composites was followed to add extra value to the properties of pure polymer, without losing its processability or adding unnecessary weight to the composite. Carbon centred nano-particles offered the prospective of combining numerous properties, such as thermal stability, mechanical strength, and electrical conductivity [1]. These excellent properties ascend from the outstanding assets of nanotubes, whose structure is based on graphene. The copiousness of graphene has made it possible for the production of efficient nano-composites. Flaw free graphene offers exceptional physical properties, such as the visual transmission of almost 98%, large specific surface area, high intrinsic mobility and ballistic transport, high thermal conductivity and Young's modulus, among others [2, 3].

The ability of a material to elastically store deformation energy and bounce back when the load is released describes its storage energy. The effective modulus of the filler describes the maximum modulus reinforcement it can possibly have in a given composite if it were to maintain the interfacial strength it manifests within the composite. Composites' storage modulus generally increases beyond the matrix value upon addition of fillers, reflecting the polymer-filler interaction, modulus of the filler, its aspect ratio, shape and size-scale. The

DOI: 10.17977/um016v5i12021p017

intimate polymer-filler interaction that arises from in situ polymerisation is expected to produce significant increases in modulus with loading [4].

Processing plays an energetic part in the production of polymer/carbon composites, and if cautiously manipulated, the inherent properties of polymers may be maintained. Additionally, the good mechanical properties and electrical conductivity of fillers such as particulate carbons can be gained by the composites/nano-composites. The anticipated gains are normally dependent on a number of factors, among which are chosen production process and the processing conditions. These two play vital roles in determining the state of the filler in a composite following compounding, including dispersion - how well the filler is reduced down to its primary particles and distribution - the distance between neighbouring filler particles within the composite and how well the positions of the particles are randomised. Poor compounding frequently leads to filler agglomeration, and the filler shows a lower aspect ratio and surface area to volume ratio.

In this research, two graphitic platelet-structured carbon fillers were used; graphite (G), an example of a micro-scale filler, and graphite nano-platelets (GNP), a comparative nano-scale filler. The size scale of the fillers is considered in fixing the level of loading with that of the GNP-based nano-composites being an order of magnitude lower than that of the G-based micro-composites. This is considered to be a better basis for comparison against the traditional [5] same-weight comparison. From an industrial position, melt blending is the favoured compounding method for the preparation of composites as it is cost-effective and environmental friendly [6]. Mixing equipment such as an extruder, and an internal mixer, can be adopted during melt blending operations.

Melt processing, which still maintains a lead in the commercial production of polymeric composites [7], was employed to make PA6/carbon composite systems over a range of loadings of G and GNP fillers. Comparing the acquired properties between melt-extruded and in situ polymerised polymer/filler composites is not new [8], but here the comparisons are more extensive. Melt extrusion was carried out using either 100/6 processing condition, which indicates an extrusion screw rotation frequency of 100 rpm applied for 6 minutes (min) or 200/3 processing conditions of 200 rpm for 3 min. Similarly, in the in situ polymerised systems G and GNP dispersion was made using two similar conditions designated as 40/10 and 20/20. Here, 40/10 indicates that sonication amplitude of 40% was applied for 10 min, whereas in the 20/20 conditions, the amplitude of 20% was applied for 20 min.

II. Material and Methods

Details experimental procedure for making the composites can be found elsewhere [9]. Since storage modulus is obtained using Dynamic Mechanical and Thermal Analysis (DMTA). DMTA is used to investigate the viscoelastic behaviour of polymers and composites by subjecting the test specimens to dynamic sinusoidal stress or strain within a temperature range, a time frame or a frequency range [10]. For viscoelastic polymers, DMTA provides useful information related to their molecular structure and relaxations [11]. A TA Instruments Q800 dynamic mechanical analyser was used to determine the thermo-mechanical responses. Specimens (approximately 5.00 x 1.55 x 17.50 mm) were cut from within the gauge length of injection moulded dog-bones made using Haake Minilab injection moulding machine. At least 3 specimens were tested for each material. The specimens were tested using a single cantilever mode and applying a Poisson's ratio of 0.35 for PA6 [12] and its composites. The tests were carried out using a temperature ramp/frequency sweep

in multi-frequency- strain operation mode, at a strain rate of 0.2 %, and a temperature ramp of 3° C/min within the region of 0-200 °C.

III. Results and Discussions

A. Storage Modulus of IG 40/10 and IG 20/20 Systems

The glass transition (Tg), storage modulus at 25 °C (E25) and storage modulus at 80 °C (E80) are presented in Table 1. Figure 1A and B is the E25 data plotted for the in situ polymerised systems, IG 40/10 and IG 20/20. E25 has more significant practical applications since amorphous and semi-crystalline composites are mainly subjected to loadings at temperatures below their Tg.

Table 1. DMTA derived storage modulus for composites in IG 40/10 (labelled-1) and IG 20/20 (labelled-2) systems

G based in situ polymerised systems	E' at 25 °C /MPa	E at 80 °C /MPa	Tg/°C (DMTA)	Tan δ at T_g X 10^{-3}
PA6	2,224±179	440±36	49.3±1.5	148±1
5G-1	2,355±393	520±130	56.7±4.0	142±6
10G-1	2,728±137	585±34	46.7±2.5	146±1
15G-1	3,052±1	750±23	53.5±2.1	143±5
20G-1	3,213±96	861±15	54.8±0.8	142±5
25G-1	2,106 ±297	695±35	32.7±5.8	136±6
5G-2	2,650±203	592±42	56.2± .1	138±2
10G-2	2,951±117	738±11	59.2±1.0	138±2
15G-2	3,213±247	837±85	57.8±2.3	134±2
20G-2	3,580±204	1001±80	59.3±1.5	138±6
25G-2	3,642±103	997±65	55.5±2.3	135±3

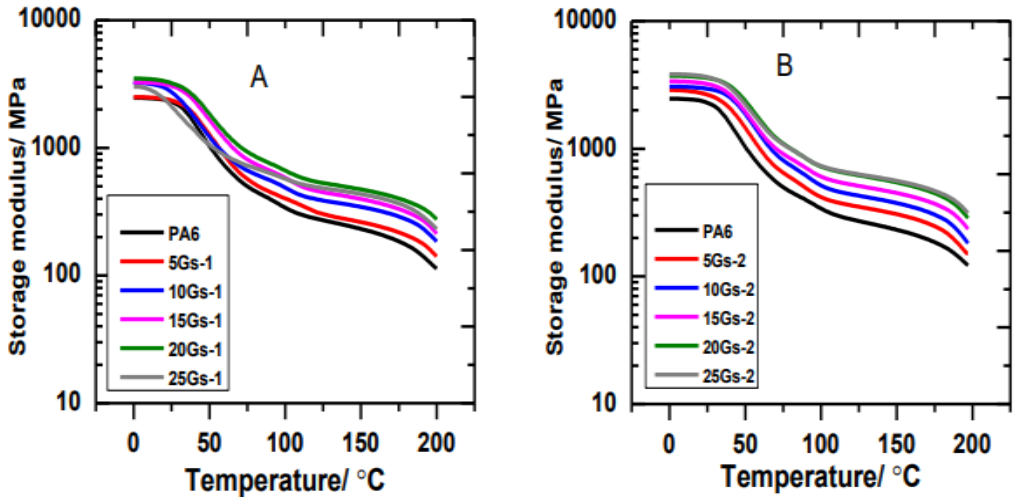

Fig. 1. Storage modulus (E') versus temperature data for (A) IG 40/10 (40% amplitude of sonication for 10 min) and (B) IG 20/20 (20% amplitude for 10 min) systems.

The storage modulus increase below Tg can be noticed from Table 1 to be more significant compared to the E80, which lays ahead of Tgbut below the melting temperature (Tm) of PA6. This behaviour concurs both with the weak interaction between G and the PA6 matrix as well as the fact that G particles are micron in size. Similar behaviour was observed when modified and unmodified montmorillonite clays were used to reinforce PA6 [13] using melt processing. The unmodified micron-sized clay composite behaved in a similar manner as observed with G.The modified nano-sized clay gave higher storage modulus at temperatures in between Tg and Tm. Relative to the unfilled PA6 forms.

The Table 1 comparison shows that the highest E25 values are obtained with the modified nano-sized (5T) clay. This is most likely attributed to the nano-scale size of the 5T modified clay and the stronger polymer/filler interaction, which is aided its ability to form H-bonds. There is a possibility that a limited H-bonding occurred with the unmodified clay (5P). Notwithstanding, all the four G based micro-composites have better E25 reinforcement compared to 5P, the unmodified clay at 5 wt. % loading. 5Gs-1 has a modulus ratio of 1.06, whereas for 5Gs-2 the highest went up to 1.19. This in all indicates that at 5G wt. % loading, the highest reinforcement occurs with the in situ polymerised IG 20/20 processing stream. This validates its better G dispersed state and relatively strong PA6/G interaction arising having the G fillers coated by PA6 as shown in the SEM micrograph presented in Figure 3.

It may be observed from Figure 2-A that composites in IG 40/10 system generally portray lower E25 compared to those in IG 20/20 system, and the traces have cross-overs, thereby delineating with G loading at the pre-Tg stage. Delineation resumes above 100 °C with the modulus traces correlating with G loading. The occurrence of the initial crossover at lower modulus reflects the difference in G dispersion between IG 20/20 and IG 40/10 systems. It is also very likely that upon softening additional particles generated in IG 40/10 migrated to form connected G aggregates which add to the modulus of the composite at higher temperatures. Previously, a loss in modulus in PA6/G systems at higher loadings was observed, and it was blamed on factors such as decreased crystallinity, reduction in spherulite dimensions and the presence of unconverted EC and of oligomers [14].

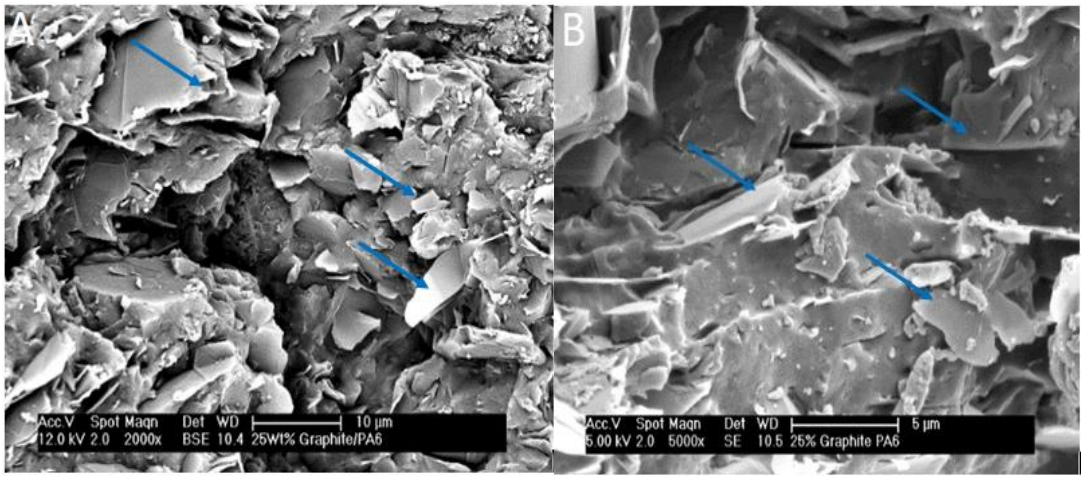

Fig. 2. SEM micrographs of PA6/G composites at 25 Gwt. % loading. A showing exposed G particulates with B showing mainly PA6 coated G particles.

B. Room Temperature Storage Moduli (E25) of the IG 40/10 and IG 20/20 Systems

Figure 3 A and B is E25 in G synthesised systems for IG 40/10 and IG 20/20 systems. In both systems, the modulus of the composites did not improve above unfilled PA6 at the lowest loading level (5G wt. %), probably because at low G loading an effective rigidity and filler connectivity [15] is yet to be met. Although in both systems, E25 generally increases with filler loading, the diverging pattern observed is interesting. In IG 40/10 the observed steep drop in modulus at the highest loading is assigned to plasticisation due to unconverted EC and low molecular weight species [16]. In the 20/20 system too, with the exception of the highest G loading (25 Gwt. %), a linear rise in modulus occurs. These observations show that at higher G loading, inhibition of the anionic polymerisation occurs. The significant fall in E25 seen in 25Gwt.% of the G 40/10 system, probably results from G inhibiting the rate of reaction arising from the increased volume of G particles generated with 40 % sonication amplitude. This increases the amount of diluents remaining with a resultant negative effect that compromises the modulus value. The inhibition of the anionic polymerisation is preventable by increasing the mole % of catalysing species [17]. The fact that the effect is so much less at the same 25 Gwt. % loading in the IG 20/20 system upholds the suggestion that a bigger fragmentation of G occurs whilst the 40/10 sonication stream is used, and this increases with G loading.

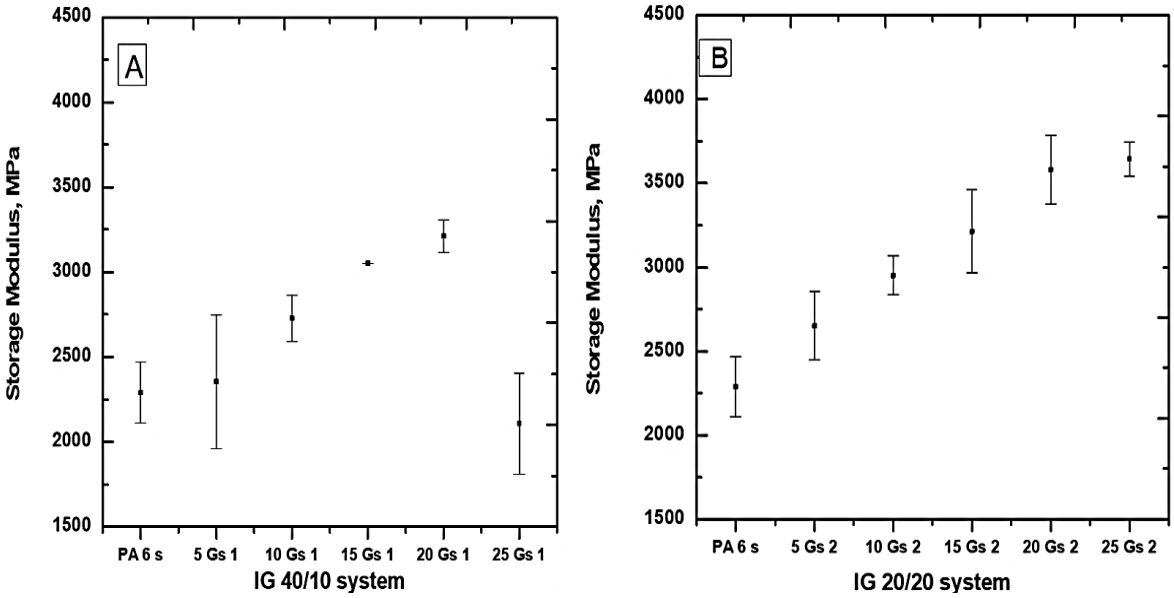

Fig. 3. A and B: E25 in G synthesised systems. IG 40/10 indicates 40% amplitude of sonication for 10 min and IG 20/20 indicates 20% amplitude for 10 min.

The effective moduli of G in both systems are estimated by linearly extrapolating to 100 wt. % G loading. In both cases, the composites' modulus value at 25 Gwt. % was excluded due to significant deviation from linearity. Excluding 25Gs-1 in the IG 40/10 system, the effective modulus of G is 7.5 GPa. Excluding 25Gs-2 in the IG 20/20 system, an effective modulus value of G of 8.9 GPa is obtained. The values obtained support the notion that G not only gets better dispersed in the IG 20/20 system but it also remains less fragmented, thereby giving a more effective reinforcement. When the data from [18] with G loading up 20 Gwt. % was subjected to the same extrapolation, an effective G modulus of 4.1 GPa was obtained.

To further assess the whether or not improvements in modulus are attained Figure 4-A and B compares normalised modulus values for the composites systems presented with some in literature. In Figure 4-A, the systems G 40/10 and G 20/20 are compared with two similar G-based synthesised systems. Horsky et al. [14] used graphite (G) as well as molybdenum disulphate (MoS2) and oil (O) in one system (described in legend as MoS2/G/O) and another system with carbon fibre (CF), G and oil described in the legend as (CF/G/O) to synthesise PA6 composites with the wt. % based on G alone. The overall best modulus enhancement is obtained in the IG 20/20 system, where steady enhancement is obtained up to 25G wt. % loading whereas, in the other systems, modulus declined at higher loadings. But at equivalent G wt. %, even IG 40/10 system did better than the literature systems. The steep drop in modulus in the CF/G/O system was blamed on the reaction inhibiting effect of CF. However, the fact that twice the amount of catalysing species were used by Horsky et al. [14] (1.2 mole % as against 0.6 mole %) and the fact that the reaction was initiated within the temperature region for maximum crystal formation (140 °C) [19, 20] and decreased side reactions [21], their products ought to have shown higher modulus since their synthesis conditions favour higher DoC [22]. Although the presence of oil as lubricant might contribute to lower the modulus, the authors assigned the decrease in modulus to weaker interactions as filler loading gets higher. The presence of low molecular weight species equally caused plasticisation, which generated voids within the composites. In the synthesised systems reported here, sonication breaks down G particles and improve its dispersion just as it also increases the tendency for G to inhibit the reaction as the loading levels becomes high. So, the drop in modulus at 25 G wt.% is not surprising and has a precedence [14]. It is important to note that this drop in modulus at 25 G wt. % concurs well with the drop in Tg. However, this is not always what obtains in literature and may be considered to be a discrepancy [5].

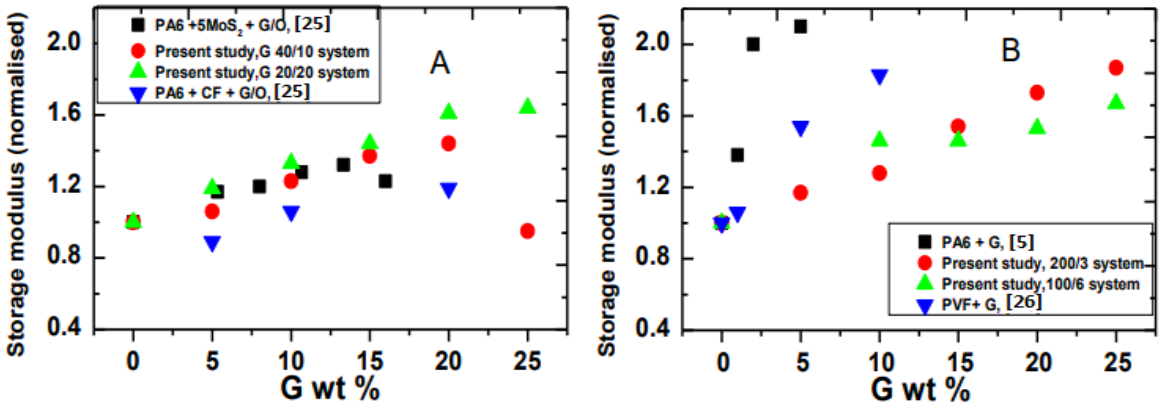

Fig. 4. A-B: Comparison of storage moduli of systems IG 40/10 (40% amplitude of sonication for 10 min) and IG 20/20 (20% amplitude for 10 min) systems) with ref.[25]. B present study with system G 200/3 and G 100/6 where(G 200/3 indicates screw speed of 200 rpm for 3 min and G 100/6 indicates screw speed of 100 rpm for 6 min), with storage moduli taken from references [5, 26]

Figure 4-B compares data for the G-based melt-processed systems presented here with literature data [23, 24]. In both G 200/3 and G 100/6 systems, modulus increases with G loading up to 25 G wt. %. The data of Ramanathan et al. [5] shows a steep increase in modulus (between 1 and 3G wt.%), followed by a levelling-off at 5 G wt.% loading, which probably indicates an onset for agglomeration. He et al. [26] observed a linear increase in

modulus without reduction up to 10 G wt. %. In both cases [5, 26], the higher modulus obtained at low G loading can be attributed to the superior filler dispersion provided by solution blending processing [6]. Due to stronger interaction, higher normalised modulus values are obtained in modified clay nano-composites, especially above Tg, where the modulus seems to collapse in the micro-composites due to the weaker and limited polymer/filler interaction. For instance, a 340% increase was obtained in a PA6/nano-clay nano-composite at 100 °C using 10 Gwt. % of modified clay while the increase at room temperature was only 86% [13].

C. Damping Behaviour of the IG 40/10 and IG 20/20 Systems

Dynamic mechanical behaviour of synthesised and melt-processed systems based on PA6 and PA6/G composites were studied. Data from the DMTA tests are given for all the systems in Table 1. Table 1 shows that greater increases in storage modulus (both at 25 and 80 °C) occur in the IG 20/20 system in comparison with IG 40/10. High storage modulus results from a good dispersion of filler in a composite, whereas increases in damping result from weak interfacial bonding [27]. Therefore, exceptional variations are not expected in the damping behaviour of these composites. Not only due to weak interaction at the filler-polymer interface but also because of the limitation in the interfacial area due to the micron size-scale of G. However, in situ polymerisation improves matrix-filler contact on the molecular scale, which in turn improves interaction [6].

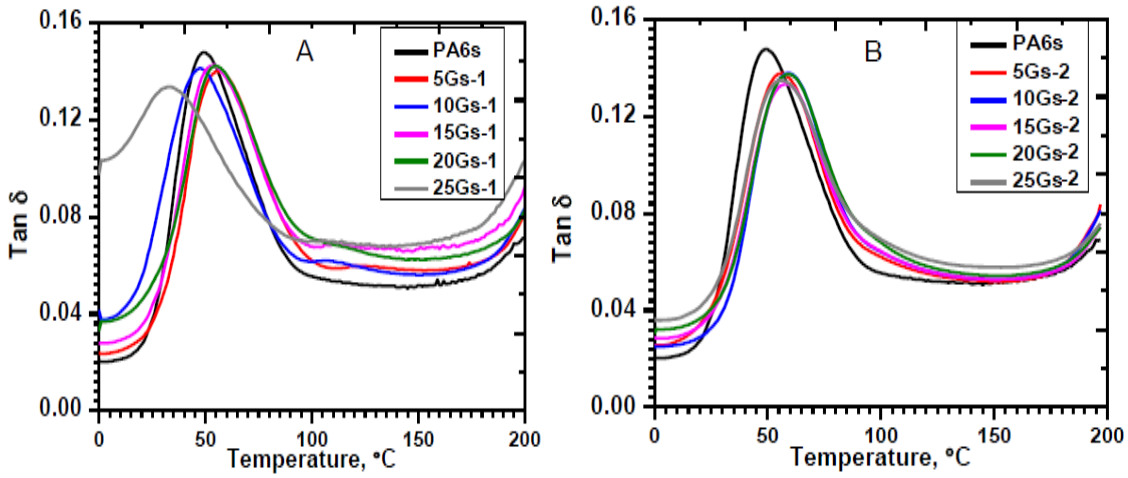

Fig. 5. Tan δ versus temperature for (A) IG 40/10 (40% amplitude of sonication for 10 min) and (B) IG 20/20 (20% amplitude for 10 min) systems.

Figure 5-A and B shows the damping behaviour of the two G-based in situ polymerised systems. In both systems, relative to the unfilled PA6, considerable damping occurs below Tg, but more damping also occurs at and above Tg in G 40/10 while in the same region, damping is only slightly greater than the unfilled in the G 20/20 system. This damping behaviour may indicate the presence of unconverted EC, low molecular weight species [14], remnants of catalysing species and even hydrogen-bonded water molecules in the composites [16]. All of these can plasticise and cause molecular motions below Tg. In a related study [14], similar damping behaviour was observed, in which damping below Tg increased with G loading (due to increased amounts of plasticising diluents), which subsequently led to reduced strength properties. This significant damping effect has to do not just with the inclusion of G but also with its loading level and dispersion. It can be observed that the unfilled PA6 has a more intense tan δ peak at Tg and narrower tan δ curves.

The composites in turn have peaks with reduced intensities which did not proportionately correspond with the increase in G loading even though, with additional G loading, more segmental chain constraint is expected. However, the relatively broader curves of the composites describe the damping behaviour resulting from the constraining effect of G on the amorphous phase.

In Figure 5-A, the IG 40/10 system has a relatively broader and less intense tan δ versus temperature traces reflecting the intensity of the amplitude of sonication used compared to IG 20/20 system. The tan δ peaks are more scattered for the IG 40/10 system, and 25Gs-1, which has the highest G loading but also has the lowest Tg (32.7±5.8 °C) as well as the lowest tan δ peak value of 136 ± 6 x 10^(-3) (Table 1). It is expected not only because it has the highest G loading but also because it has the highest DoC. Having the highest DoC and at the same time having the highest G loading shows the nucleating effect of G. In addition, the low Tg and high pre-Tg damping suggests that it is a low molecular weight product with high proportion of low molecular weight species [28]. Horsky et al. [14] got Tg values of not more than 21°C for similar composite systems and even for the unfilled PA6. These Tg values were recovered to 55 °C by washing the product.

In the G 40/10 system, further support of the effect of sonication amplitude is the appearance of broad shoulders on the tan δ peaks between 90-145 °C for the composites. The intensity of these shoulders seems to decrease with G loading, and therefore the shoulder appears most faintly in 25Gs-1. More clearly defined peaks (shoulders) were observed in clay-based composites of PA6, which were assigned to the merger of associating constrained amorphous phases [13, 29]. Therefore, these shoulders may indicate softening of this constrained amorphous phase [28, 30] at higher temperatures, similar to the interpretation of Tsagaropoulous and Eisenberg [31].

In the IG 20/20system, the composites' tan δ responses are close together, although relative to unfilled PA6 the peaks are less intense and are relatively broader indicating limited interfacial interaction. The order in terms of the height of the tan δ peak, the lowest of which describes the most restrained composite, is 15Gs-2 followed by 25Gs-2. Whereas 20Gs-2, 10Gs-2 and 5Gs-2 have practically the same tan δ height (values in Table 1).

Therefore, taking G loading the order in tan δ peak value within the system's composites' is consistent and suggests that G is better distributed in PA6. This correlates well with the rise in Tg of 10 °C between PA6 and 20Gs-2. Furthermore, the rise in the composites' Tg, E25 and modulus at 80 °C between composites of parallel loading in IG 40/10 and IG 20/20 systems confirm the same.

Changes in the damping behaviour of polymers upon adding foreign particles occur with diverse effects on Tg, which is sometimes taken as an indicator for good interaction [5]. For example, Milliman et al. [32] co-blended PA6 with polyhedral oligomeric silsesquioxane (POSS) up to 10 wt. % loading. Increased damping occurred above 1wt. % POSS loading. However, the best improvements in modulus occurred at 2.5 wt. % loading, and at the same time, Tg rose by 15 °C due to strong interactions. No further improvements occur with further loadings due to phase separation. However, increased damping followed by a reduction in Tg implied good interaction in the case of modified clays [13] due to the release of organic diluents intercalated within the clay galleries upon exfoliation. Again, anionic polymerisation of EC with MWCNT led to reduced Tg, and increased damping though higher modulus values were obtained with loading due to good dispersion [33].

IV. Conclusions

The storage and effective moduli of four PA6/G composite systems were investigated and compared. Two, which are G 40/10 and G 20/20 systems, were in situ polymerisation based where theoretically equivalent G dispersion strain of 400 was used. In the other two systems, G 100/6 and G 200/3, melt extrusion was used. An extrusion strain theoretically equivalent to 600 was used to disperse G in molten PA6. The storage moduli were evaluated at 25 ºC (E25) and 80ºC (E80). The composite/unfilled PA6 ratios of E25 and E80 for the in situ polymerised system IG 40/10 are 1.37 and 1.63, respectively. For the in situ polymerised system IG 20/20, the E25 and E80 ratios were respectively 1.96 and 2.28. This gave the IG 20/20 system superior thermo-mechanical property amongst the in situ polymerised systems. For the melt-extruded systems, G 100/6 had lower E25 and E80 ratios of 1.67 and 2.03 as against the G 200/3 system, where the ratios were respectively 1.87 and 2.64. While the better storage modulus values shown in the G 200/3 melt-extruded system is associated with the lesser extrusion duration, which significantly reduced any tendency to thermal decay, the better storage modulus properties exhibited by G 20/20 in the in situ polymerised system is associated with the enhanced filler connectivity network that improved heat dissipation The effective modulus for the in situ polymerised systems IG 40/10 and IG 20/20 were 7.5 GPa and 8.9 GPa while that of melt-extruded systems G200/3 and G100/6 tallied at 8.2 GPa. All the results indicate that the G 20/20 processing conditions produced composites with the best thermo-mechanical properties.

Nomenclature

PA6	: Nylon 6
G	: Graphite
IG	: *in situ* polymerised graphite
E25	: Storage Modulus at $25^{o}C$
E80	: Storage Modulus at $80^{o}C$
IG 40/10	: Sonication amplitude of 40% applied for 10 min.
IG 20/20	: Sonication amplitude of 20% applied for 20 min.
G 100/6	: Melt extrusion screw rotation frequency of 100 rpm applied for 6 min.
G 200/3	: Melt extrusion screw rotation frequency of 200 rpm applied for 3 min.
GNP	: Graphite Nano-platelets
DMTA	: Dynamic Mechanical and Thermal Analysis
EC	: Epsilon Caprolactam
DoC	: Degree of Conversion
POSS	: Polyhedral Oligomericsil Sesquioxane
Tan δ	: Storage Modulus
T_g	: Glass transition temperature
T_m	: Melting temperature
MoS_2/G/O	: Molybdenum disulphate (MoS_2), Graphite (G) and oil (O)
CF/G/O	: Carbon Fibre (CF), Graphite (G) and oil (O)
5G-1	: 5 % weight of G relative to EC for IG 40/10 system
10G-1	: 10 % weight of G relative to EC for IG 40/10 system
15G-1	: 15 % weight of G relative to EC for IG 40/10 system
20G-1	: 20 % weight of G relative to EC for IG 40/10 system
25G-1	: 25 % weight of G relative to EC for IG 40/10 system
5G-2	: 5 % weight of G relative to EC for IG 20/20 system
10G-2	: 10 % weight of G relative to EC for IG 20/20 system

15G-2 : 15 % weight of G relative to EC for IG 20/20 system
20G-2 : 20 % weight of G relative to EC for IG 20/20 system
25G-2 : 25 % weight of G relative to EC for IG 20/20 system

References

[1] Vaia, R. A., and Wagner, H. D."Framework for nanocomposites", *Materials Today,* vol. 7(11), 32–37, 2004.

[2] Rao, C. N. R., Biswas, K., Subrahmanyam, K. S., and Govindaraj, A., "Graphene, the new nanocarbon", *Journal of Materials Chemistry,* 19(17), pp. 2457–2469, 2009.

[3] Soldano, C., Mahmood, A., and Dujardin, E. "Production, properties and potential of grapheme",*Carbon,* vol. 48(8), pp. 2127–2150, 2010.

[4] Verdejo, R., Bernal, M.M., Romasanta, L.J., and Lopez-Manchado, M.A."Graphene filled polymer nanocomposites", *Journal of Materials Chemistry,* vol. 21(10), pp. 3301-3310, 2011.

[5] Ramanathan, T., Stankovich, S., Dikin, D.A., Liu, H., Shen, H., Nguyen, S.T., and Brinson, L.C."Graphitic nanofillers in PMMA nanocomposites-an investigation of particle size and dispersion and their influence on nanocomposite properties", *Journal of Polymer Science Part B: Polymer Physics,* vol. 45(15), pp. 2097-2112, 2007.

[6] Sengupta, R., Bhattacharya, M., Bandyopadhyay, S., Bhowmick, A. K. "A review on the mechanical and electrical properties of graphite and modified graphite-reinforced polymer composites", *Progress in Polymer Science*, vol. 36(5), 638-670, 2011.

[7] Hussain, F., Hojjati, M., Okamoto, M., and Gorga, R. E. "Review article: polymer-matrix nanocomposites, processing, manufacturing, and application: an overview", *Journal of composite materials,* vol. 40(17), pp. 1511-1575, 2006.

[8] Tung, J., Gupta, R., Simon, G., Edward, G., and Bhattacharya, S. "Rheological and mechanical comparative study of in situ polymerised and melt-blended nylon 6 nanocomposites" *Polymer,* vol. 46(23), pp. 10405-10418, 2005.

[9] Umar, M., Ofem, M.I., Anwar, A.S., and Salisu, A.G. "Thermogravimetric analysis (TGA) of PA6/G and PA6/GNP composites using two processing streams. *Journal of King Saud University - Engineering Sciences. https://www.sciencedirect.com/science/article/pii/S1018363920302968* (2020)

[10] Menzel, J.D., and Prime, R.B *"Thermal analysis of polymers: Fundamentals and Applications"*, John Wiley & Sons Inc 2009

[11] Campbell, D., Pethrick, R.A., and White, J.R.*"Polymer Characterisation:Physical Techniques"* Taylor & Francis, Second Edition ed. 2000.

[12] Shen, L. Phang, I.Y., and Liu, T. "Nanoindentation studies on polymorphism of nylon 6", *Polymer testing,* vol. 25(2), pp. 249-253, 2006.

[13] Wilkinson, A.N., Man, Z., Stanford, J.L., Matikainen, P., Clemens, M.L., Lees, G.C., and Liauw, C.M. "Structure and dynamic mechanical properties of melt intercalated polyamide 6-montmorillonite nanocomposites", *Macromolecular Materials and Engineering,* vol. 291(8), pp. 917-928, 2006.

[14] Horský, J. Kolařík, J.,and Fambri. L. Structure and Mechanical Properties of Composites of Poly (6-hexanelactam) Combining Solid Tribological Additives and

Reinforcing Components. *Macromolecular Materials and Engineering,* vol. 289(4), pp. 324-333, 2004.

[15] Kim, H.and Macosko, C.W. "Processing-property relationships of polycarbonate/graphene composites", *Polymer,* vol. 50(15), pp. 3797-3809, 2009.

[16] Kolařík, J. and Janáček. J. "Secondary (β) Relaxation Process of Alkaline Polycaprolactam Swollen by Low Molecular Weight Substances", *Journal of Polymer Science Part C: Polymer Symposia.* 1967. Wiley Online Library

[17] Ahmadi, S., Morshedian, J., Hashemi, S., Carreau, P., and Leelapornpisit, W."Novel Anionic Polymerization of ε-Caprolactam Towards Polyamide 6 Containing Nanofibrils", *Iranian Polymer Journal*, vol. 19(3), pp. 229-240, 2010.

[18] Horský, J. Kolařík, J., and Fambri. L."Composites of alkaline poly(6-hexanelactam) with solid lubricants: one-step synthesis, structure, and mechanical properties", *Die Angewandte Makromolekulare Chemie, vol.* 271(1), pp. 75-83, 1999.

[19] Udipi, K., Davé, R.S., Kruse, R.L., and Stebbins, L.R."Polyamides from lactams via anionic ring-opening polymerisation: 1. Chemistry and some recent findings", *Polymer,* vol. 38(4), pp. 927-938, 1997.

[20] Davé, R.S., Kruse, R.L., and Stebbins, L.R., and Udipi, K."Polyamides from lactams via anionic ring-opening polymerisation: 2. Kinetics" *Polymer,* vol. 38(4), pp. 939-947, 1997.

[21] Ueda, K., Yamada, K., Nakai, M., Matsuda, T., Hosoda, M., and Tai, K. "Synthesis of high molecular weight nylon 6 by anionic polymerisation of ε-caprolactam", *Polymer Journal*, vol. 28(5), pp. 446-451, 1996.

[22] Rijswijk, K. van, Bersee, H.E.N., Jager, W.F., and Picken, S.J."Optimisation of anionic polyamide-6 for vacuum infusion of thermoplastic composites: choice of activator and initiator", *Composites Part A: Applied Science and Manufacturing*, vol. 37(6), pp. 949-956, 2006.

[23] Clingerman, M.L."*Development and modelling of electrically conductive composite materials*", PhD Thesis, 2001, Michigan Technological University.

[24] Clingerman, M.L., Weber, E.H., King, J.A., Schulz, K.H"Synergistic effect of carbon fillers in electrically conductive nylon 6, 6 and polycarbonate-based resins", *Polymer Composites,* vol. 23(5), 911-924, 2002.

[25] Gubbels, F., Blacher, S., Vanlathem, E., Jerome, R., Deltour, R., Brouers, F., and Teyssie, Ph."Design of electrical composites: determining the role of the morphology on the electrical properties of carbon black filled polymer blends", *Macromolecules,* vol. 28(5), pp. 1559-1566, 1995.

[26] He, F., Fan, J., and Lau, S."Thermal, mechanical, and dielectric properties of graphite-reinforced poly (vinylidene fluoride) composites" *Polymer Testing,* vol. 27(8), pp. 964-970, 2008.

[27] Ma, P.C., Siddiqui, N.A., Marom, G., and Kim, J.K. "Dispersion and functionalisation of carbon nanotubes for polymer-based nanocomposites: a review", *Composites Part A: Applied Science and Manufacturing*, vol. 41(10), pp. 1345-1367, 2010.

[28] Ning, N., Fu, S., Zhang, W., Chen, F., Wang K, Deng H, Zhang, Q., and Q. "Realising the enhancement of interfacial interaction in semicrystalline polymer/filler composites

via interfacial crystallisation" *Progress in Polymer Science,* vol. 37(10), pp. 1425-1455, 2012.

[29] Shelley, J., Mather, P., and DeVries, K. "Reinforcement and environmental degradation of nylon-6/clay nanocomposites", *Polymer,* 42(13):5849-5858, 2001.

[30] Priya, L., and Jog, J. "Poly (vinylidene fluoride)/clay nanocomposites prepared by melt intercalation: Crystallisation and dynamic mechanical behavior studies", *Journal of Polymer Science Part B: Polymer Physics.*40(15), pp. 1682-1689, 2002.

[31] Tsagaropoulos, G., and Eisenberg, A. "Dynamic mechanical study of the factors affecting the two glass transition behaviour of filled polymers. Similarities and differences with random ionomers", *Macromolecules,* vol. 28(18), pp. 6067-6077, 1995.

[32] Milliman, H. W., Ishida, H., and Schiraldi, D.A. "Structure property relationships and the role of processing in the reinforcement of nylon 6-POSS blends", *Macromolecules,* vol. 45(11), pp. 4650-4657, 2012.

[33] Kelar, K., and Jurkowski B. "Properties of anionic polymerised ε-caprolactam in the presence of carbon nanotubes", *Journal of Applied Polymer Science,* vol. 104(5), pp. 3010-3017, 2007.